COMBINING WATER VAPOR DATA FROM GPS AND MERIS.

Roderik Lindenbergh, Maxim Keshin, Hans van der Marel and Ramon Hanssen
Delft Institute of Earth Observation and Space Systems, Delft University of Technology
r.c.lindenbergh@tudelft.nl

KEY WORDS: GPS, MERIS, Kriging, water vapor, spatial-temporal

ABSTRACT

Improved knowledge of atmospheric water vapor and its temporal and spatial variability is of great scientific interest for climate research and weather prediction, but also geodetic positioning applications using GPS and radar interferometry will benefit. In this article a comparison is made of MERIS and GPS based integrated water vapor data, retrieved at the same day over Western Europe. For both signals a variance-covariance analysis is made, that will be applied in producing a time series of combined water vapor maps by means of the geostatistical Cokriging approach.

1 INTRODUCTION

Water vapor is the atmosphere's dominant greenhouse gas. Besides accounting for a large part of Earth's natural greenhouse effect, gaseous water also condenses to form clouds, which act as an isolation layer for earth's surface temperature. Knowledge on water vapor values is not only essential for environmental issues but also for satellite measurements from GPS and (In)SAR: the GPS or SAR signal will be delayed by the water vapor while traveling through the atmosphere. Unlike most other atmospheric gases, the distribution of water in the atmosphere varies strongly with time, location and altitude. This makes it necessary to monitor it at both high spatial and high temporal resolution. Mapping the spatial distribution of water vapor in the atmosphere is difficult due to the limited spatial and temporal resolution of contemporary meteorological instrumentation.

It is however also possible to retrieve water vapor estimations from satellite systems. In this paper two systems are considered. At ground stations from the world wide Global Positioning System (GPS), the zenith Integrated Water Vapor (IWV) can be derived from the total delay that the GPS signals undergo while traveling from the GPS satellites to the GPS receiver at the ground stations. This derivation results in relative good IWV estimates with a high temporal (e.g. 1 hour) but a low spatial resolution (tens to hundreds kilometers). The MERIS instrument on the Envisat satellite estimates integrated water vapor by observing the backscatter of solar radiation in the near infrared over land, sea and above clouds. With a maximum spatial resolution of 300 m, MERIS can observe dynamic structures on scales much smaller than possible before. It's temporal resolution however is restricted to 3 days.

For this article we will compare and combine the GPS and MERIS data sets as introduced above. For this purpose a variance-covariance analysis will be made for the data sets, both based on the specifications of the data providers and on an experimental analysis. This step will result in a listing of the major error components for both cases. In the MERIS case this analysis will be only spatial, in the GPS case it will be temporal as well. The two data sets will be combined to produce a time series of combined hourly water vapor maps by means of incorporating individual and cross-covariances into a Cokriging system, (Goovaerts, 1997). Except for the water vapor maps itself, this procedure will result in error maps, displaying the errors as propagated from the individual data error components. These results will give a clear insight in the gain that is expected from combining GPS and MERIS water vapor data.

2 GPS AND MERIS IWV DATA

2.1 Integrated Water Vapour

Water vapor is the gas phase of water. Gaseous water represents a small but environmentally significant constituent of the atmosphere. Most of it is contained in the boundary layer, the lowest 2[km] of the troposphere. In this article we will consider columnar water vapor values. Such values are expressed in [kg/m^2], that is as the mass of the water vapor contents in a column of atmosphere above a horizontal square patch of 1[m] $\times$ 1[m] on the Earth's surface.

The change in IWV above a fixed point of the Earth's surface can to some extend be described by Taylor's frozen flow assumption, (Taylor, 1938). This hypothesis states that a random field, in our case the water vapor distribution, as a whole is transported by the mean wind. As wind velocities and directions vary with their height above the Earth's surface, Taylor's assumption is of only limited use for direct assessment of Integrated Water Vapour Values. It is reported, (Elgered et al., 2005), that IWV fields often significantly change while traveling one hour upwind.

Knowledge on water vapor values is not only essential for environmental issues but also for satellite measurements from GPS and (In)SAR: the GPS or SAR signal meets the water vapor while traveling through the atmosphere and will be delayed by it.

2.2 GPS IWV

In GPS data processing, measurements from all satellite signal paths are mapped onto the vertical direction by means of a pre-defined mapping function. In this way the effect of GPS signal propagation delay above a GPS station can be estimated. This effect is called the zenith tropospheric path delay. Only the total effect can be directly estimated from GPS measurements in this way, although in general

it consists of two components. The first, hydrostatic, component reflects the impact of dry air on the propagation of the GPS signal and depends on the surface pressure. The second, wet, component appears due to the presence of water vapor in the lower parts of the atmosphere. Therefore, the zenith total delay (ZTD) can be decomposed into two parts: Zenith Hydrostatic Delay (ZHD) and Zenith Wet Delay (ZWD), that is,

$$\text{ZTD} \;=\; \text{ZHD} + \text{ZWD}. \tag{1}$$

ZHD can be computed directly as follows

$$\text{ZHD} \;=\; \frac{0.0022767 \cdot P}{1 - 0.00266\cos 2\varphi - 2.8 \cdot 10^{-7} H}, \tag{2}$$

where φ is the ellipsoidal latitude of the GPS station, H the orthometric station height and P the surface pressure. ZWD is then obtained from Equation 1. Zenith wet delay can then be mapped into integrated precipitable water vapor (IWV) by means of the following expression:

$$\text{IWV} \;=\; \Pi \cdot \text{ZWD}, \tag{3}$$

where Π is about 0.15 and depends on the mean temperature of the atmosphere, (Bevis et al., 1994, Klein Baltink et al., 2002).

GPS IWV processing. ZTD's can be estimated along with many other parameters, such as station coordinates, using different GPS software packages, for instance, the Bernese software or GIPSY. This process can be performed both in near real-time and in post-processing mode with time resolutions down to 5-6 min. Numerous validation experiments showed that an accuracy of 1-2 $\mathrm{kg/m^2}$ IWV is achievable for both post-processed and near real-time GPS IWV estimates, (Jarlemark et al., 2002, Klein Baltink et al., 2002, Elgered et al., 2005). The possibility to use data from GPS networks for operational meteorology has been demonstrated in the framework of the COST-716 action (Elgered et al., 2005), which took place in 2001-2004. In 2003, the period under consideration in this paper, ten European Analysis Centers were participating in that action, which involved processing a network of more than 350 stations covering the whole of Europe.

GPS footprint. The IWV at a given GPS station at a given time is determined from a number of different signal paths, one for every visible GPS satellite. If the GPS-IWV estimate is compared to MERIS measurements of 300[m] or 1[km] spatial resolution, an obvious question is what to take for the footprint size and shape of the GPS-IWV estimate. As the configuration of GPS satellites is continuously changing it is at first approach only possible to use an approximate footprint. We assume that the footprint is circular, which is in general not correct, as less GPS satellites will be available to the North of the GPS ground station, on high northern latitudes. Instead of using a geometric approach depending on elevation cutoff, we obtained an optimal radius R_{GPS} as follows: Let R vary between 0 and a suitable upper limit of in our case 25[km] and determine for every value of R the correlation coefficient between the GPS-IWV estimates and the MERIS-IWV pixels within distance R of the GPS stations. That value of R that gives the highest correlation is chosen as the footprint radius R_{GPS}.

2.3 MERIS IWV

Since its launch on board the Envisat satellite in March 2002, the Medium Resolution Imaging Spectrometer MERIS gives insight into the properties and dynamics of the Earth system with unprecedented accuracy and resolution. MERIS is a push-broom imaging spectrometer with a spatial resolution of 300m. It measures the solar radiation reflected by the Earth in 15 spectral bands, programmable in width and position, in the visible and near infra-red. The main mission of MERIS is oceanography, observing sea-color. The secondary mission of MERIS is to observe, amongst others, the water vapor column over land, water or above clouds. Observations are limited to the day-side. Global coverage is obtained after 3 days. MERIS also retrieves cloud type and top height.

Integrated Water Vapour values are obtained by a differential absorption method from the radiances L_{14} and L_{15} measured in channels 14 and 15, resp., (Bennartz and Fischer, 2001). These channels are centered around 890 and 900 [nm], with a half width value of ± 5 [nm]. The ESA algorithm to derive the IWV estimates, W, is based on the logarithmic relation

$$W \;=\; k_0 + k_1 \log \frac{L_{15}}{L_{14}} + k_2 \log^2 \frac{L_{15}}{L_{14}}, \tag{4}$$

between the columnar water vapor and the ratio of the spectral radiances from bands 15 and 14. The k_0, k_1 and k_2 are regression constants.

The values of the regression constants depend on the viewing geometry. But, there are also differences in methodology for IWV estimates above land and water, (Fischer and Bennartz, 1997). The absorption of water is higher, therefore the aerosol scattering gains influence and is taken into account over water by including the values for the 'aerosol' channels 9, 12, and 13 in the determination of the regression constants. The theoretical accuracy of the estimated water vapor column is 1.7 [$\mathrm{kg/m^2}$] over land and 2.6 [$\mathrm{kg/m^2}$] over water at full resolution, (Bennartz and Fischer, 2001). The specified accuracy for the IWV contents at the reduced resolution of 1.2 km is specified by ESA as smaller than 20%.

3 INTEGRATING GPS AND MERIS DATA.

3.1 Kriging and Cokriging.

Spatial and temporal continuity Correlation in time or in space between observations can be detected and modeled by a variogram or covariance analysis, (Goovaerts, 1997). The resulting model is used to determine the variance-covariance matrices of the observations. Using the VC-matrices, a Best Linear Unbiased Prediction can be obtained for the IWV content at a given time and location.

The underlying assumption used in this framework is that the signal, in our case the IWV, can be considered a random function. This means that every observation is one single outcome of a complete distribution of possible observations at that time and location. Stationarity of a random function means that the function is independent of location or time.

Covariance analysis The theoretical covariance function of a stationary random function $Z(x)$ is defined as

$$\text{cov}(s) \quad = \quad E\{Z(x) - m\}\{Z(x+s) - m\}, \quad (5)$$

where $m = E\{Z(x)\}$ denotes the mean of $Z(x)$ and s a temporal or spatial distance. Given a set of observations, a discrete experimental covariance function can be determined by computing experimental covariances between any two observations and by grouping the outcomes according to some distance interval. By fitting the experimental values into a positive definite model, a continuous covariance function is obtained that is used to fill the VC-matrix for a prediction at arbitrary location or moment.

4 DATA DESCRIPTION AND COMPARISON.

The position of all data considered here is given in WGS84 (World Geodetic System 1984) coordinates, that is, the position of a data point is given by a latitude and a longitude with respect to the WGS84 reference ellipsoid. Distances between points are spheroidal and are computed along (approximate) great circles with respect to this ellipsoid. Time is given in Coordinated Universal Time (UTC), which corresponds to the time zone of Greenwhich on the western part of the scene considered.

4.1 GPS data.

The GPS data we used is originating from the 26 GPS COST-716 ground stations, as shown in Fig. 1. We used as much data as possible from one processing center, therefore 24 stations were taken from the GeoForschungsZentrum (GFZ) in Potsdam. Two additional stations processed by the Nordic Geodetic Commission (NKG), were added to improve the spatial coverage. For the given list of stations we consider all available IWV data from August 9, 2003. For the GFZ stations mostly IWV estimates are available at quarter past and quarter before the whole hour, but some data are missing. NKG data is available at 15 minutes interval, but here data points are missing as well.

4.2 Processing the MERIS data.

We used one MERIS reduced resolution product, acquired at August 9, 2003, between 10:11:27 and 10:14:44 UTC. At reduced resolution, one pixel is available for every 1.2×1.2 km^2 at nadir direction.

Data flags. A MERIS Level 2 data set contains an *Integrated Water Vapor* attribute. The value of this attribute at a given position may not always be representing the actual IWV value, due to e.g. the presence of cloud cover. Therefore a filter step is necessary. Except for several data attributes, the MERIS Level 2 product also provides a quality attribute consisting of a flag number. The binary representation of this flag number consists of a list of 24 zeroes and ones. A one indicates that a certain boolean operator is TRUE.

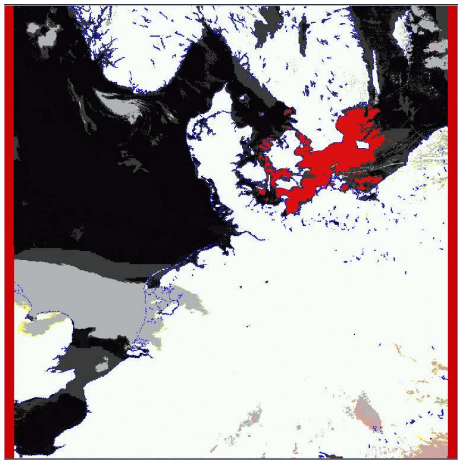

Figure 2: Classification according to MERIS flags. Clearly visible are the land (white), water (black) and coastline pixels (blue). 'Uncertain total water vapor content' is indicated in red, clouds in light gray and 'cloud, snow or ice over land' pixels are in yellow. These pixels were removed from the MERIS data set.

We removed IWV points for which the CLOUD flag, the PCD_14 flag, or the TOAVI_CSI flag is true, see Fig. 2. The CLOUD flag indicates that a cloud product is available; the PCD_14 flag indicates that the total water vapor content is uncertain while the TOAVI_CSI flag indicates Cloud, Snow or Ice over land pixels, according to MGVI processing. For our test data set this filter step reduces the number of points in the scene from 1 256 641 to 1 090 222 points. The other flags were ignored. At the moment it is not clear if this is the best way of filtering.

4.3 Comparison at MERIS time.

Single pixel comparison. After removal of suspicious MERIS points, a comparison was made between the GPS IWV values at MERIS acquisition time and the values of the remaining MERIS pixels close to the GPS stations. First the MERIS pixel closest to each of the GPS stations was determined, see Fig. 3. The correlation between these GPS and MERIS estimates is only 0.627. This bad correlation value is mainly caused by some strong outliers. Especially near Stavanger, Oberpfaffenhofen, Pfaender and, to a lesser degree, near Braunschweig and Helgoland, agreement in estimates is small. Therefore the MERIS pixels around these GPS stations were considered in detail.

Local situation around GPS stations. In Fig. 4 the values of 25 MERIS pixels are shown around four GPS stations with values deviating from the nearby MERIS pixel values. The situation around GPS station Oberpfaffenhofen is not considered, as the most close MERIS pixel after the filtering step of above is already at 10.9 [km] dis-

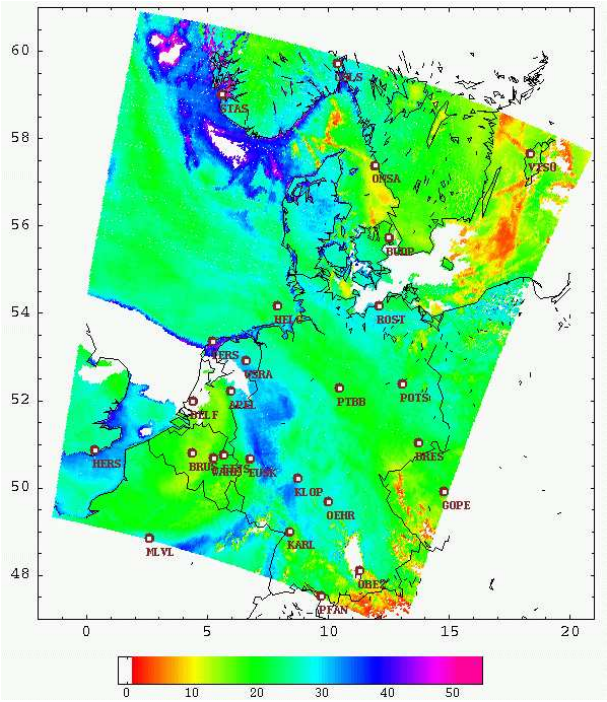

GPS Code	Site Name	Proc. center
APEL	Apeldoorn	GFZ
BRUS	Brussel	GFZ
BUDP	Kbenhavn	GFZ
DELF	Delft	GFZ
DRES	Dresden	GFZ
EIJS	Eijsden	GFZ
EUSK	Euskirchen	GFZ
GOPE	Pecny,Ondrejov	GFZ
HELG	Helgoland	GFZ
HERS	Herstmonceux	GFZ
KARL	Karlsruhe	GFZ
KLOP	Kloppenheim	GFZ
MLVL	Marne-La-Vallee	GFZ
OBE2	Oberpfaffenhofen	GFZ
ONSA	Onsala	GFZ
OEHR	Oehr	GFZ
OSLS	Oslo	NKG
PFAN	Pfaender	GFZ
POTS	Potsdam	GFZ
PTBB	Braunschweig	GFZ
ROST	Rostock-Warnemuende	GFZ
STAS	Stavanger	NKG
TERS	Terschelling	GFZ
VIS0	Visby	GFZ
WARE	Waremme	GFZ
WSRA	Westerbork	GFZ

Figure 1: MERIS water vapor data from August 13, 2003, ± 10:00 o'clock. The MERIS data will be compared and combined with water vapor data from the 26 indicated GPS ground stations.

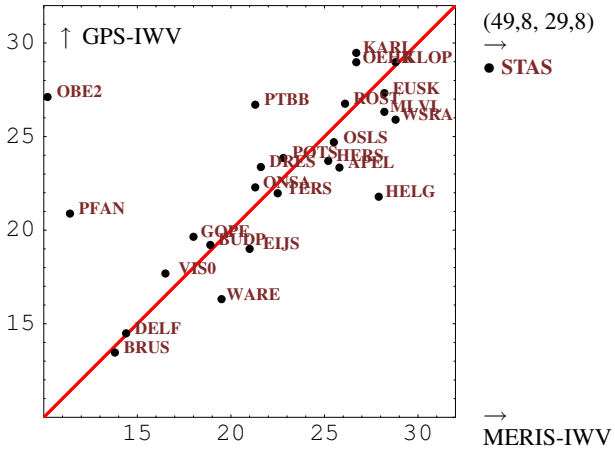

Figure 3: IWV values at GPS stations and at most close MERIS pixel.

tance. Around three stations we observe big jumps between neighboring MERIS pixels: in all three cases jumps of more than 5 [kg/m^2] exist. Around Stavanger even a jump can be found from 25.8 [kg/m^2] to 49.8 [kg/m^2]. An explanation for these jumps can be found in the MERIS flags.

Near the Braunschweig station two single flags, 'LAND' and 'PCD_19', are true for all pixels and those pixels all have similar values. Around Helgoland we see more variability in the MERIS pixel values, and in the flags as well. In this case however it is not true that for pixels with similar values the same flags are true. What should be noted in this case that all pixels are marked as 'water', so the existence of the two small islands of in total 1.7 [km^2] that form Helgoland cannot be found back on the MERIS image.

Around Pfaender we find both 'LAND' and 'WATER' pixels. All MERIS pixels with relative high values are 'LAND' pixels. Intermediate values are found at 'LAND' pixels that are marked as 'COASTLINE' pixels as well. Around Stavanger the situation is the other way around. Here the 'WATER' pixels have high values compared to the 'LAND' pixels. Both in the Pfaender and the Stavanger case however the values of the 'LAND' pixels are most close to the IWV value as determined by th nearby GPS station.

Correlation MERIS-GPS vs. GPS footprint size. After determining correlation for different footprint sizes of the GPS estimates, as described in Section 2.2, it was found that maximal correlation occurs for R_{GPS} = 1.75 [km]. For this footprint of about 10 km^2 the GPS-MERIS correlation equals 0.79. Using this radius implies that the about 8 MERIS pixels most close to a GPS station were used in the correlation comparison. It should still be checked whether this radius is in good correspondence with the true GPS cut-off elevation angle of about 10 degrees.

A correlation of 0.853 is obtained if stations are disregarded with a maximal difference of more than 5 kg/[m^2] between the MERIS pixels within the GPS footprint. In this way the stations of Onsala, Pfaenders, Stavanger and Terschelling (all coastal!) are removed from the comparison because of big jumps, while Delft and Oberpfaffen-

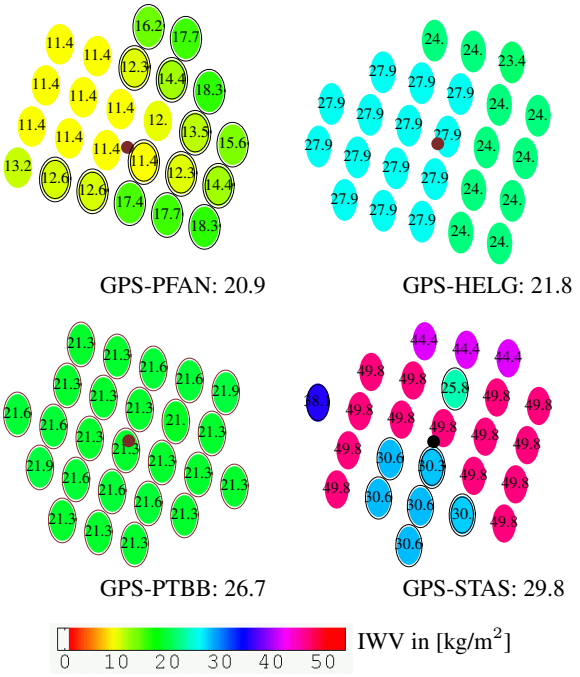

Figure 4: IWV values at 25 MERIS pixels most close to a GPS station. Top left: Pfaender. Top right: Helgoland. Bottom left: Braunschweig. Bottom right: Stavanger. 'LAND' pixels are surrounded by one circle, 'COASTLINE' pixels by two circles.

hofen have no MERIS data to compare within the GPS footprint.

4.4 Data correlation.

GPS spatial correlation As the number of different GPS station considered is only 26, it is difficult to determine a reliable covariogram for the spatial correlation at a single epoch Therefore a spatial experimental covariogram is determined from the, if necessary, linearly interpolated GPS measurements at every hour between 0.30 and 23.30. These epoch times are chosen because for most GPS stations and most epochs, IWV estimates are available at exactly the half hours. The covariogram for 10:30 is shown in dark blue in Fig. 5, left. Only those interpolated GPS IWV values were used for the hourly covariograms for which at least one measurement is available within one hour of the covariogram time. The mean of the experimental covariograms obtained in this way is shown in red in Fig. 5, left. This covariogram displays a range, i.e. the maximal distance at which correlation exists, of about 200km and this approximately holds for all individual covariograms as well. The sill, or more precise, the average experimental covariance within the first bin of 60km of the individual covariograms however is highly variable during the day, and varies from 40 at 00:30 downwards to -10 at 06:30 and then again upwards via 50 at 10:30 (figure) up to 90 at 15:30, in order to end at 23:30 at a value of 65. This shows that the size of the spatial covariance of the IWV signal as measured by GPS is highly variable with time although it's range seems more stable. A more elaborated approach can be found in (de Haan et al., 2005).

MERIS spatial correlation The experimental covariogram of a subset of about 1100 MERIS IWV observations is given in blue in Fig. 5, left. Here a bit smaller bin width of 10km is used. This covariogram is fairly comparable to the covariogram of the GPS IWV data of 10:30. Due to the higher spatial resolution, the range of the MERIS covariogram is higher than the GPS range and is equal to almost 500km.

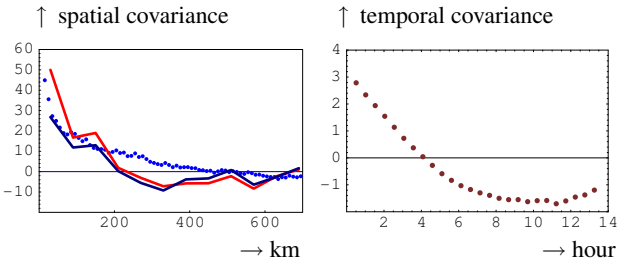

Figure 5: Covariograms of the IWV data. Left: spatial. In dark blue: GPS covariogram at 10:30. In red: mean of 24 hourly spatial GPS covariograms. In blue: covariogram of the MERIS data. Right: temporal. Mean of the 26 temporal covariograms of the detrended IWV values at the different GPS stations.

GPS temporal correlation The time series of the GPS IWV at the different GPS ground stations display a strong trend. Therefore a linear trend was fitted at each station and removed from the data. The mean of the 26 temporal covariance functions, determined from the detrended data is given by the brown dots in Fig. 5, right. As the IWV values at most stations even show some non-linear trend during the day, the stationarity condition for the random function does not hold very well. This is expressed by the negative covariance values at higher distance.

Combining the MERIS and GPS data. When producing IWV maps from the GPS IWV observations, the additional MERIS observations can be used in two different ways. First of all, the MERIS observations are directly incorporated in producing the maps by means of the Cokriging approach. For this purpose the individual VC-matrices of both the GPS and the MERIS observations are needed together with the cross-correlation VC-matrix containing the cross-covariances between the MERIS and GPS observations.

Moreover, the MERIS IWV observations can be used to gauge and control the covariance parameters of the GPS IWV observations. Here, this approach is sketched and illustrated by means of inverse distance interpolation, but the approach can be used in exactly the same way for the Kriging method. This procedure is illustrated in Fig. 6, where two maps of the spatial IWV distribution at MERIS time are shown. The left map is based on the MERIS observations and is obtained by a nearest neighbor interpolation to a 0.25×0.1 degree longitude-latitude grid. Here, the nearest neighbors from each of the eight octants around a grid-point are used to produce a grid-point prediction. Note that in comparison to Fig. 1 all smaller gaps have

been filled. Grid points for which no observation is available in all eight octants within 100 km did not get a value.

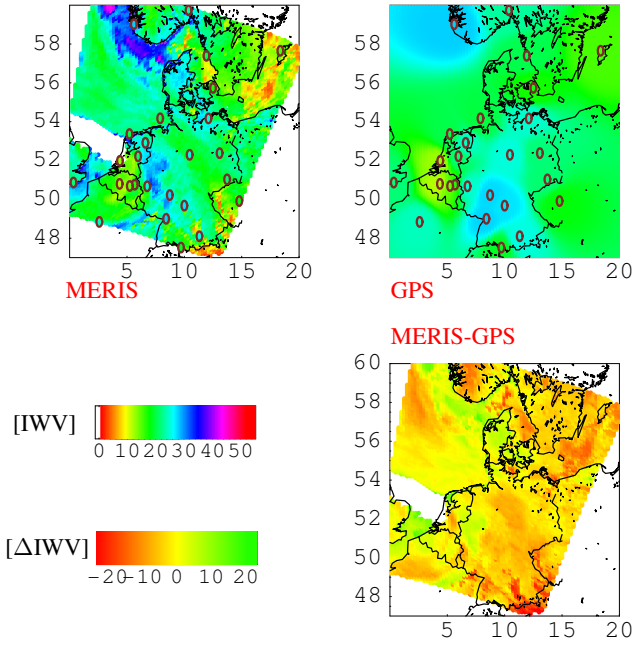

Figure 6: Interpolated MERIS (top-left) and GPS (top-right) observations at MERIS time. Both data sets are interpolated to the same grid. At the bottom the difference between the two maps is given.

Optimizing the GPS IWV prediction. On the top right of Fig. 1 the same grid is filled by inter- and extrapolated values based on the estimated GPS observations at the 26 GPS station near MERIS time. Here a inverse distance interpolation is used with a high power (p=5) in order to give observations a long influence range. The bottom right shows the difference between the MERIS and GPS maps. The mean absolute difference equals 4.1 [kg/m^2]. By varying the parameters for the GPS IWV interpolation, different mean absolute difference values are found. Optimal prediction parameters are obtained when the mean absolute difference value is minimal. This approach can be used to gauge a prediction method like inverse distance but can also be applied for finding optimal parameters for Kriging.

5 CONCLUSIONS AND FURTHER RESEARCH.

In this paper it is sketched how to combine GPS and MERIS IWV observations.

This combination will be executed in near future. The quality of a combined map at a given time can be assessed by performing a cross-validation with GPS IWV observations from around that time. Moreover, a quality description will be directly obtained from the variances and covariances as they propagate in the Cokriging/Best linear unbiased prediction procedure. Of course both quality descriptions should be compared and combined.

The MERIS IWV algorithm uses different methods above land and water. This causes large differences between IWV values of neighboring MERIS pixels far beyond the specified accuracy. A further analysis of near-coastal IWV values may lead to an improvement of the current algorithms as used by MERIS for processing IWV data.

For our particular setting we found a correlation of 0.79 when comparing the IWV observation at a GPS station with the average of the MERIS IWV pixels within a radius of 1.75 [km]. This shows that the reported accuracies of the MERIS and GPS IWV observations are consistent. It is recommended however to further determine an optimal footprint shape and size for the GPS IWV observations following either the method sketched in this paper or by a geometrical method, but in both cases by using larger amounts of e.g. MERIS data.

These first results were obtained with observations of only one day. Currently we are in process of testing larger data sets.

Acknowledgments.

Sybren de Haan from KNMI is thanked for providing the authors with the GPS IWV data and for his useful comments. The MERIS data is distributed by ESA. This project is funded under number EO-085 by the Netherlands Institute for Space Research, SRON.

REFERENCES

Bennartz, R. and Fischer, J., 2001. Retrieval of columnar water vapour over land from back-scattered solar radiation using the medium resolution imaging spectrometer (MERIS). Remote Sensing of Environment 78, pp. 271–280.

Bevis, M., Businger, S., Chiswell, S., Herring, T., Anthes, R., Rocken, C. and Ware, R., 1994. GPS Meteorology: Mapping Zenith Wet Delays onto Precipitable Water. J Appl Meteor 33, pp. 379–386.

de Haan, S., van der Marel, H., Gündlich, B. and Barlag, S., 2005. Resolving spatial and temporal atmospheric water vapour structures using a ground based gps receiver network. Technical Report project EO-050, SRON.

Elgered, G., Plag, H.-P., van der Marel, H., Barlag, S. and Nash, J., 2005. Exploitation of ground-based GPS for operational numerical weather prediction and climate applications, Final report. Technical report, COST Action 716, European cooperation in the field of scientific and technical research.

Fischer, J. and Bennartz, R., 1997. Retrieval of total water vapour content from MERIS measurements, algorithm theoretical basis document. Technical Report PO-TN-MEL-GS-0005, ESA-ESTEC, Noordwijk, Netherlands.

Goovaerts, P., 1997. Geostatistics for Natural Resources Evaluation. Oxford University Press.

Jarlemark, P., Johansson, J., Stoew, B. and Elgered, G., 2002. Real time GPS data processing for regional atmospheric delay. Geophys. Res. Lett. 29(16), pp. 7/1–4.

Klein Baltink, H., van der Marel, H. and Van der Hoeven, A. G. A., 2002. Integrated atmospheric water vapor estimates from a regional GPS network. Journal of Geophysical Research 107(D3), pp. 4025, doi:10.1029/2000JD000094.

Taylor, G. I., 1938. The spectrum of turbulence. Proceedings Royal Society London, Series A 164, pp. 476–490.

Appendix A. GPS IWV observations at 26 ground stations.

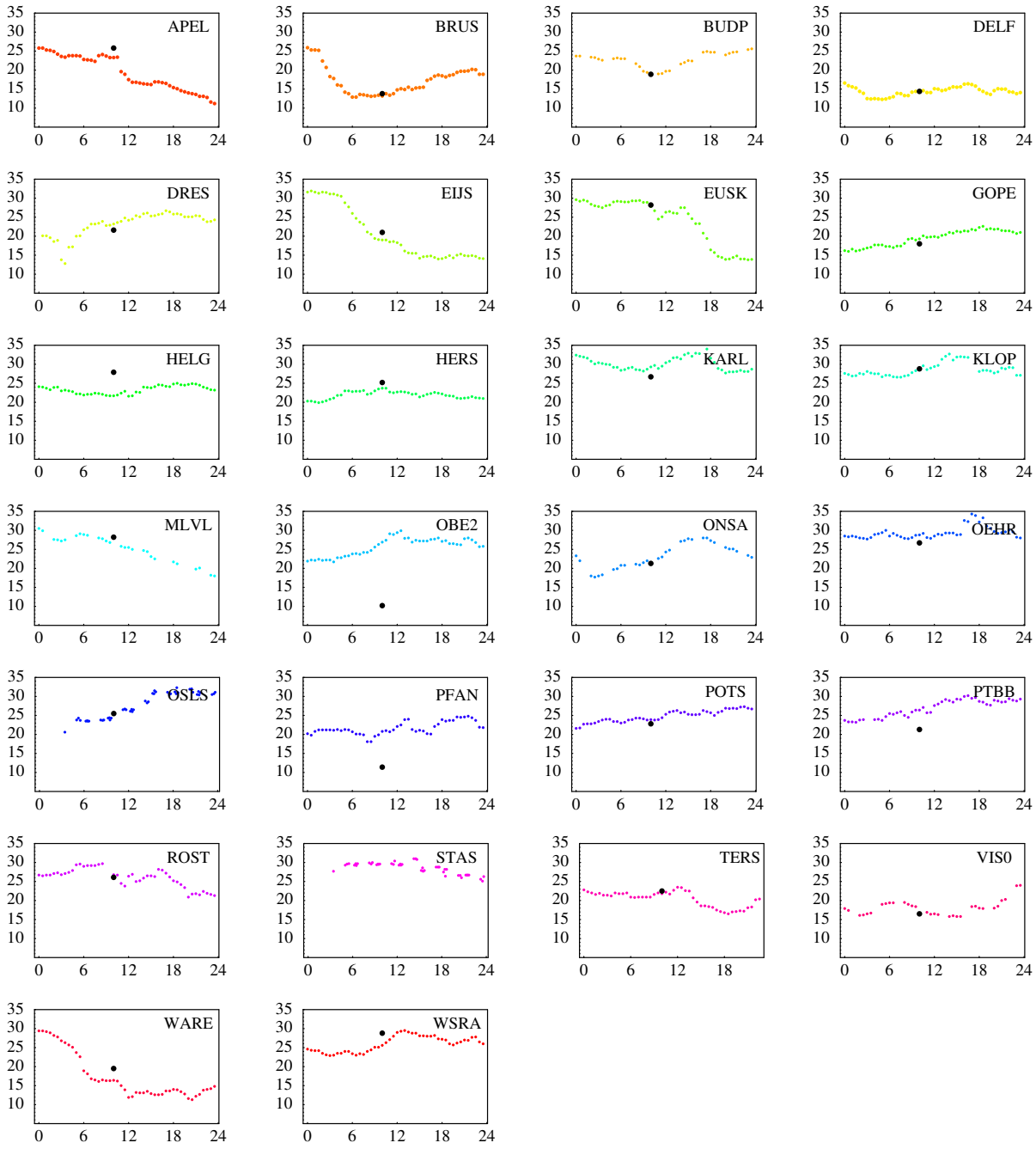

Figure 7: Time series of GPS IWV measurements of the different GPS ground stations. For each station the value of the most close MERIS IWV pixel is indicated by a black dot at MERIS time.

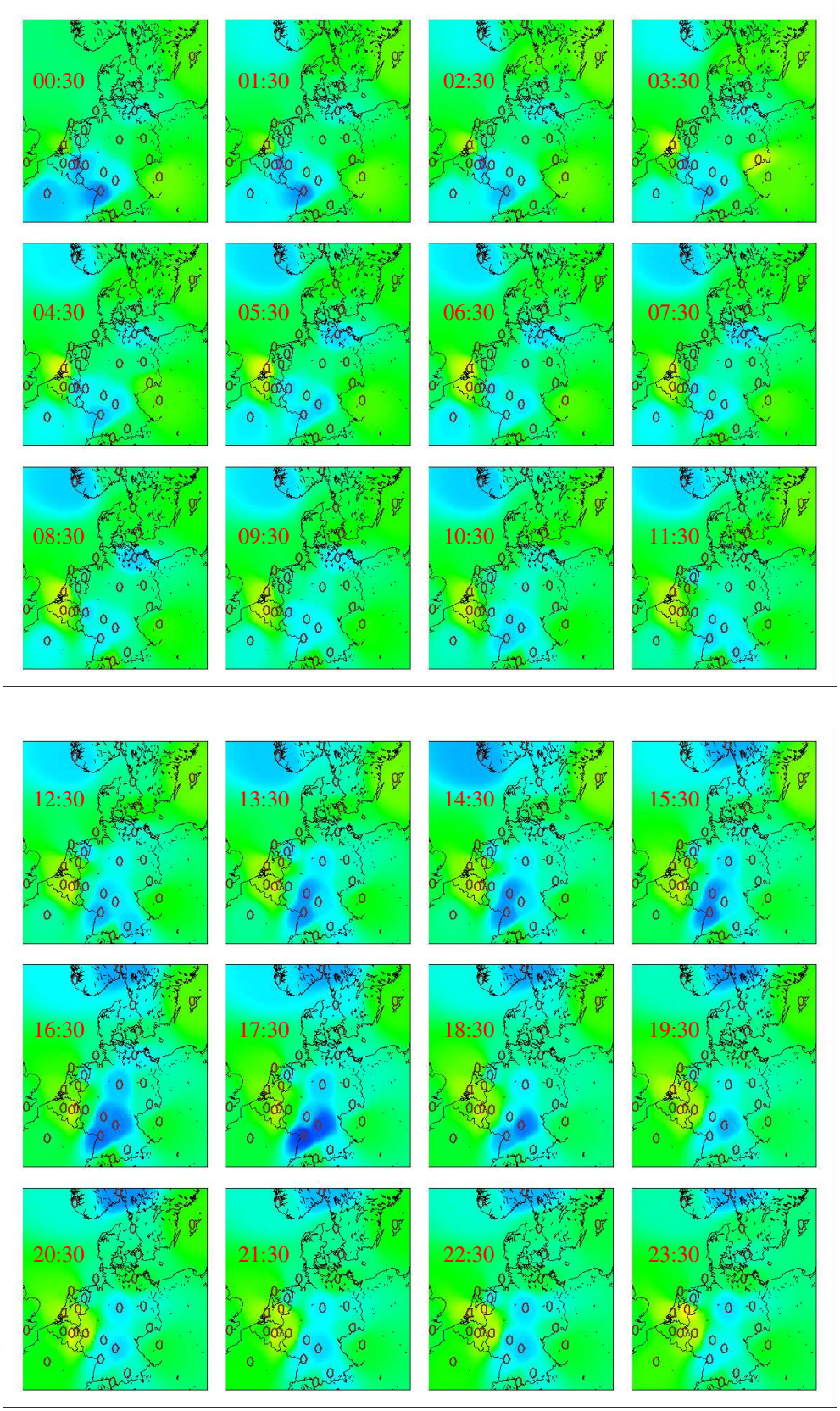

Figure 8: Hourly maps of interpolated GPS-IWV observations.